Rock Mechanics and Rock Engineering (2022) 55:1361–1374
https://doi.org/10.1007/s00603-021-02715-5

ORIGINAL PAPER

New Insights into Failure Behaviors of Tectonic Coal Under Triaxial Conditions Using Reconstituted Coal Specimens

Jia Lin[1,4] · Yuanping Cheng[1,2,3] · Ting Ren[4] · Qingquan Liu[1,2,3] · Qingyi Tu[5]

Received: 20 May 2021 / Accepted: 9 November 2021 / Published online: 30 November 2021

Abstract

Coal and gas outburst is tightly related to the existence of tectonic coal. Because large blocks of tectonic coals are difficult to be collected, reconstituted coal specimens are often used to study the mechanical properties. In this study, reconstituted coal specimens were prepared under different external forces. Then, triaxial compression tests were conducted under different confining pressures. The deviatoric stress, volumetric strain, axial strain and dilatancy ratio were analyzed. From the laboratory tests, the cohesion of reconstituted coal is positively related to the applied external force. Bonds are developed between coal particles. It is found that the deviatoric stress mainly contributes to bond breakage and internal friction. Under low confining pressure testing condition, the specimen is in over-consolidation state. The failure process is similar to the failure of intact coal. The deviatoric stress reaches the peak value. Then a strain-softening effect is observed with the bond breakage. But for normal consolidation scenario, the bond-breakage stress is smaller than the maximum internal friction force. With the increase of deviatoric stress, the shear stress exceeds the threshold limit value of bond breakage first and then, it exceeds the maximum internal force. Before the new unstable fracture development, extensive bond breakage happens. When the shear stress exceeds the maximum friction force, internal slippage occurs with sharp increases of dilatancy ratio. From this study, the failure behaviors of reconstituted coal are closely related to the stress conditions. The understanding of tectonic coal failure process is enhanced.

✉ Jia Lin
jl562@uowmail.edu.au

✉ Yuanping Cheng
ypcheng@cumt.edu.cn

[1] National Engineering Research Center for Coal Gas Control, China University of Mining and Technology, Xuzhou 221116, Jiangsu, China

[2] Key Laboratory of Gas and Fire Control for Coal Mines (China University of Mining and Technology), Ministry of Education, Xuzhou 221116, China

[3] School of Safety Engineering, China University of Mining and Technology, Xuzhou 221116, Jiangsu, China

[4] School of Civil, Mining and Environmental Engineering, University of Wollongong, Wollongong, NSW 2500, Australia

[5] State Key Laboratory of Mining Response and Disaster Prevention and Control in Deep Coal Mines, Anhui University of Science and Technology, Huainan 232001, China

Highlights

- Reconstituted coal samples were prepared under different external forces and were tested under triaxial confining-conditions.
- The stress dilatancy relationship is established and dilatancy ratio is quantified.
- The deviatoric stress contributes to the internal friction and bonds breakage for the consolidated specimen.
- Based on the OCR (overconsilidation ratio), different failure mechanisms were found for the reconstituted coals.

Keywords Tectonic coal · Reconstituted coal · Consolidation · Bond breakage · Dilatancy

List of Symbols

q	Deviatoric stress
σ_1	Maximum principal stress, axial stress
σ_2	Intermediate principal stress
σ_3	Minimum principal stress, confining stress
ε_1	Axial strain
ε_3	Radial strain
ε_v	Volumetric strain
τ	Shear stress
c	Cohesion of the specimen
φ	Internal friction angle
UCS	Uniaxial compression strength
E	Young's modulus
μ	Poisson's ratio
d	Dilatancy ratio
ε_v^p	Plastic volumetric strain
ε_s^p	Plastic shear strain
η	Normalized stress decrease percentage
N_p	Normalized stress at the peak state
N_r	Normalized stress at the end of the test
OCR	Over-consolidation ratio
ΔW_f	Frictional loss work
ΔW_b	Bond breakage work
p	Mean stress
M	Critical-state stress ratio
σ_{bb}	Bond breakage stress
σ_{mf}	Maximum friction stress
f	Friction force
k	Internal friction force coefficient

1 Introduction

Coal and gas outbursts cause several damages to underground mining activities. The outburst events have been recorded for a long period of time in many coalfields (Harvey and Singh 1998; Karacan et al. 2011; Lama and Bodziony 1998). The understanding of outburst is enhanced with the development of coal mining industry and it is generally regarded that there are mainly three key factors for coal and gas outburst: high in situ stress, high seam gas content and geological structure (Fan et al. 2020; Lama and Bodziony 1998; Wold et al. 2008). It was previously found the geological structure does not contribute to the outburst, but the tectonic coal does (Cheng and Pan 2020).

Tectonic coals are generated during the development of geological structures. The structure of the coal is damaged by the geological movement and pieces or coal powders are formed. Under the high in situ stress conditions, these damaged coals are compacted and consolidated and the tectonic coals are generated. From field observation, the tectonic coal is usually distributed near the structures, like fault, dyke intrusion, or near the interface between coal and rock (Anyim and Gan 2020; Cheng and Pan 2020; Frodsham and Gayer 1999). For tectonic coal, the strength is low and the cohesion is weaker than the intact coal (Dong et al. 2018). The permeability of tectonic coal is much lower than the regular coals because the gas drainage performance is unsatisfactory (Zhao et al. 2021b). Low gas flow is observed when the gas drainage borehole is drilled into the tectonic coal (Jia et al. 2019).

Many researchers investigate the characteristics of tectonic coals. The porosity is studied and compared between intact coals and tectonic coals from the same coal seam. It is found that there is no significant difference between tectonic coals and intact coals for the total pores volume and the internal specific area (Qu et al. 2010). The sorption capacities of tectonic coal and intact coal are studied. It found that the difference is also not significant (Chen et al. 2017). That means the micro-pores are not damaged by the tectonic movements (Qu et al. 2010). The coal seam gas is mainly stored in the micropores as sorption state. The macro-pores and fracture system in the coal are destroyed. The diffusion process is also studied and different results are observed. There are no consistent findings for tectonic coals (Yu et al. 2020). It should be pointed out that the above characterization tests are based on the pulverized coal. These above parameters of the tectonic coal can be well represented by the coal powders (Jin et al. 2016). The mechanical properties are usually studied in laboratory through cylindrical specimen or cubic specimen (Skoczylas et al. 2014). The tectonic coal is very brittle and fragile. Large tectonic coal blocks cannot be collected, and in the laboratory, the standard cylindrical coal specimen cannot be obtained. The method of investigating the mechanical properties of tectonic coal is different from that of the intact coal or rock. The coal particles (smaller than 5 mm) are used for the uniaxial compression test. The effective elastic modulus and tensile strength can be calculated (Dong et al. 2018). A comparison is made between tectonic coal and intact coal and it finds that the strength of tectonic coal is much weaker than intact coal. Even though this method can be used to measure the mechanical properties, the interactions between in situ stress and the physical properties cannot be studied. Meanwhile, the failure behavior cannot represent the in situ coal seam failure behavior.

The reconstituted coal sample is used widely to study the mechanical response under triaxial stress conditions (Chen et al. 2013; Liu et al. 2017). The preparation process of reconstituted coals is various and there is no consistent standard for sample preparations. For example, water and/or cement are used as the additives with different percentage

(P. G et al. 2012). The external applied forces are different. There are no specific guidelines for the sample preparations. Therefore, the relationship between the sampling preparation parameters and the in situ tectonic coal's (Young's modulus, UCS, cohesion) is not developed. In other words, the reconstituted coals cannot accurately represent the tectonic coal in particular coal seams. From the seepage aspect, the reconstituted coal's permeability measured in the laboratory would be two or three orders of magnitude higher than the in situ tectonic coal's permeability (Liu et al. 2018). This clearly demonstrates that the reconstituted coal is not fully replicated from the in situ tectonic coal. The preparation of reconstituted samples is very similar to the soil/clay consolidation process (Wang and Leung 2008; Wu et al. 2021). The soil particles are compacted and consolidated with/without drainage under triaxial stress conditions. The mechanical strength and failure behaviors are studied. Compared with the soil consolidation process, the preparation of reconstituted coal is regarded as drained-consolidated process, because the water percentage is relatively low and far from saturation. The confining stress and consolidation stress are much higher for reconstituted coals.

In this study, the reconstituted coal specimens were prepared under two different external applied forces (100 KN and 200 KN). Triaxial compression tests were conducted under different confining pressures. From the testing results (different confining pressures), the failure behaviors of the reconstituted specimens are compared. It is observed that the transition pressure (from brittle to ductile) is different. The deviatoric stress, volumetric strain, dilatancy ratio and axial strain were analyzed. Based on the specimen's stress history, the consolidated status was established for each sample. The relationship between the confining pressure (sample preparation process) and the mechanical properties is established. The failure behaviors were analyzed by the integration of stress and dilatancy effect.

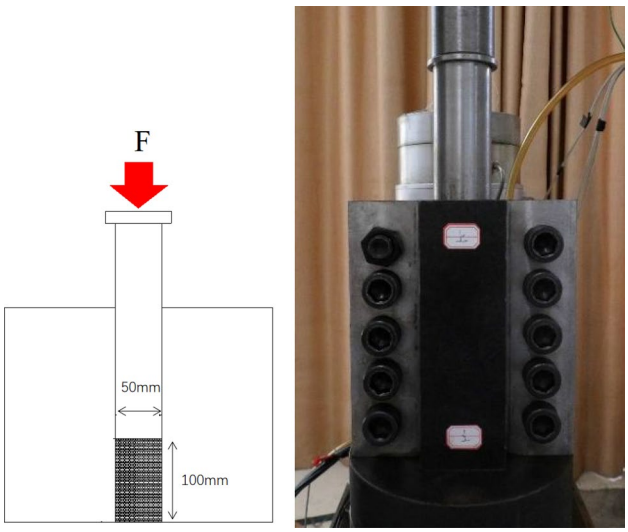

Fig. 1 Schematic diagram and photo of the split cylinder mold

2 Materials and Methods

Small coal blocks of soft coals were collected from geological structure zones from Huainan coalfield, China. These coal blocks were crushed and milled into coal powders. The particles with size smaller than 1 mm were screened and chosen for the reconstituted coal preparation. The coal particles were first mixed with water (with weight percentage of 6%) and then casted into a split cylinder mold, as shown in Fig. 1. External forces were applied on the top end face. Cylindrical coal specimens with the size 50 mm in diameter by 100 mm in length were produced. In this study, two groups of reconstituted coal specimen were prepared under different external forces: 200 KN and 100 KN (Liu et al. 2017; Tu et al. 2019). For the convenience, the samples produced by 200 KN external force were marked as Group I and by 100 KN external force marked as Group II. The external force was increased gradually with the loading rate of 300 N/s. When the targeted force was reached, it was maintained for another 3 h. Then, the specimens were cured in a vacuum oven at 60 ℃ for 24 h.

The triaxial mechanical-permeability testing rig is used for the triaxial testing. During the mining process or the tunnel excavation process, the in situ stress path is different from the stress path in this study. The rock mass or coal seam experience loading–unloading stress path. The excavation process transfers the stress into the rock mass or coal in front of the excavation face. In this study, only the stress loading process is investigated. No stress unloading tests are conducted. The main purpose of this study is to study the failure behavior of the tectonic coal during stress loading process. The axial and confining loading were supplied through a hydraulic oil servo system. The maximum axial

Table 1 Testing no. for Group I and Group II

Testing no.	Testing group	External force (preparation process)	Confining pressure, MPa
1	Group I	200 KN	2
2	Group I	200 KN	4
3	Group I	200 KN	6
4	Group I	200 KN	8
5	Group II	100 KN	1
6	Group II	100 KN	2
7	Group II	100 KN	4
8	Group II	100 KN	6

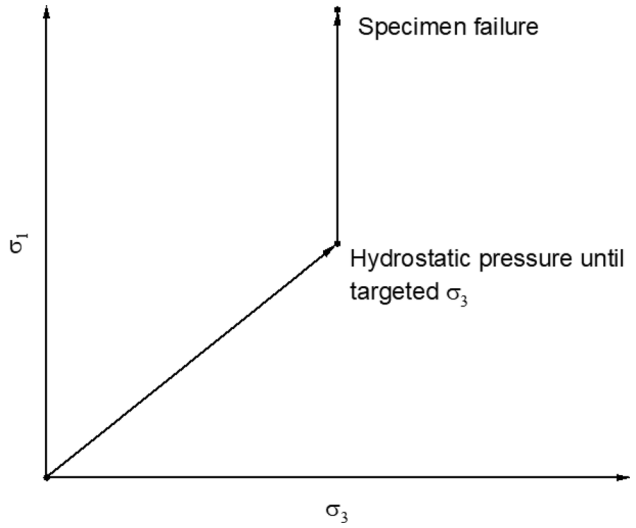

Fig. 2 Stress path of testing: axial stress σ_1, confining stress σ_3

and confining loading are 300 MPa and 60 MPa, respectively. More detailed illustration regarding this triaxial testing system can be found in previous studies (Chen et al. 2013; Liu et al. 2018). In this study, conventional triaxial loading tests were conducted under different confining pressures. For the specimens produced under the external force of 100 KN, the confining pressures were 1, 2, 4 and 6 MPa; for the specimens produced under the external force of 200 KN, the confining pressures were 2, 4, 6 and 8 MPa, as shown in Table 1. The axial stress and confining stress were loaded at the same rate of 10 N/s until the confining pressure reached the targeted value. Then the axial loading was applied at the rate of 50 N/s to the end of the test while the confining pressure was kept constant at the targeted value. The loading path of the testing is shown in Fig. 2.

3 Testing Results

3.1 Deviatoric Stress and Volumetric Strain

Two curves including the deviatoric stress ($q = \sigma_1 - \sigma_3$) with respect to the axial strain (ε_1) and the volumetric strain (ε_v) with respect to the axial strain (ε_1), are shown in Figs. 3 and 4. It can be seen that first the deviatoric stress increases linearly, reaching the maximum value, and then

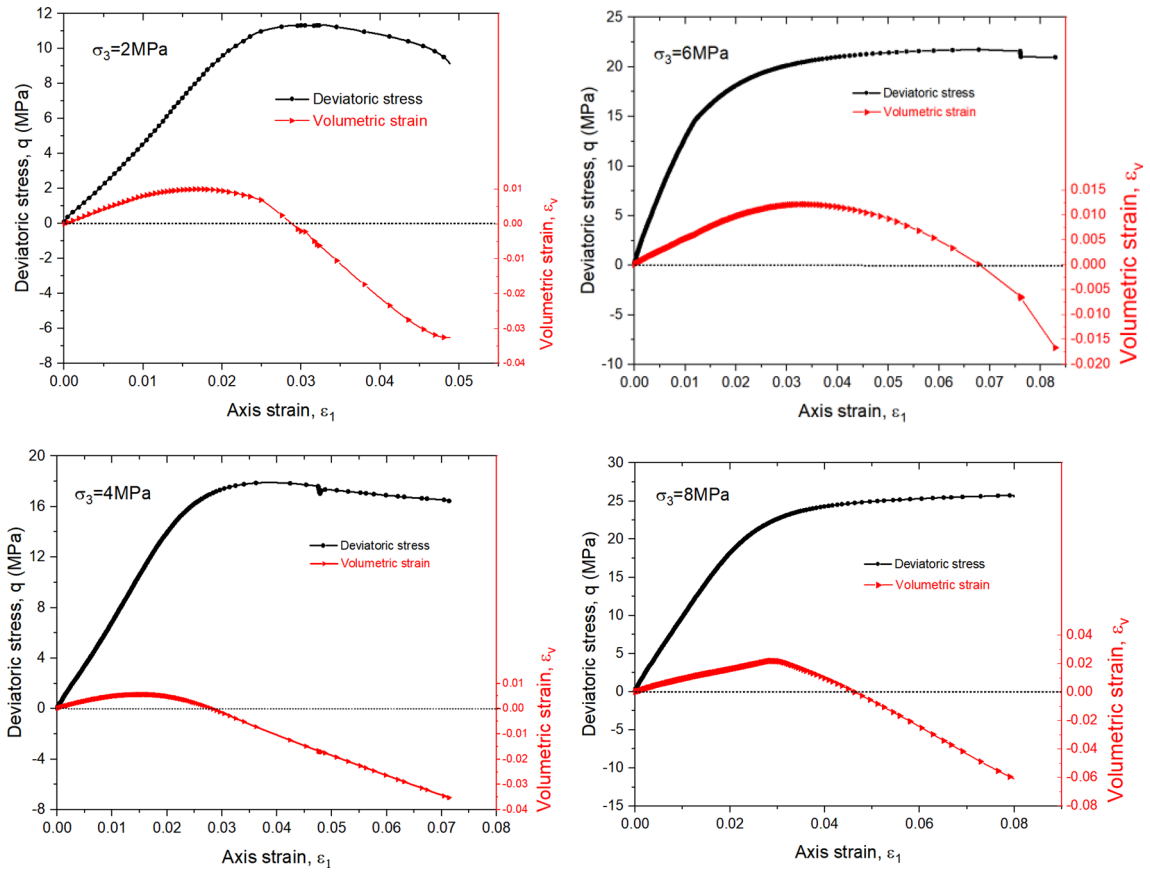

Fig. 3 Deviatoric stress and volumetric strain with respect to axial strain under different confining pressures for Group I

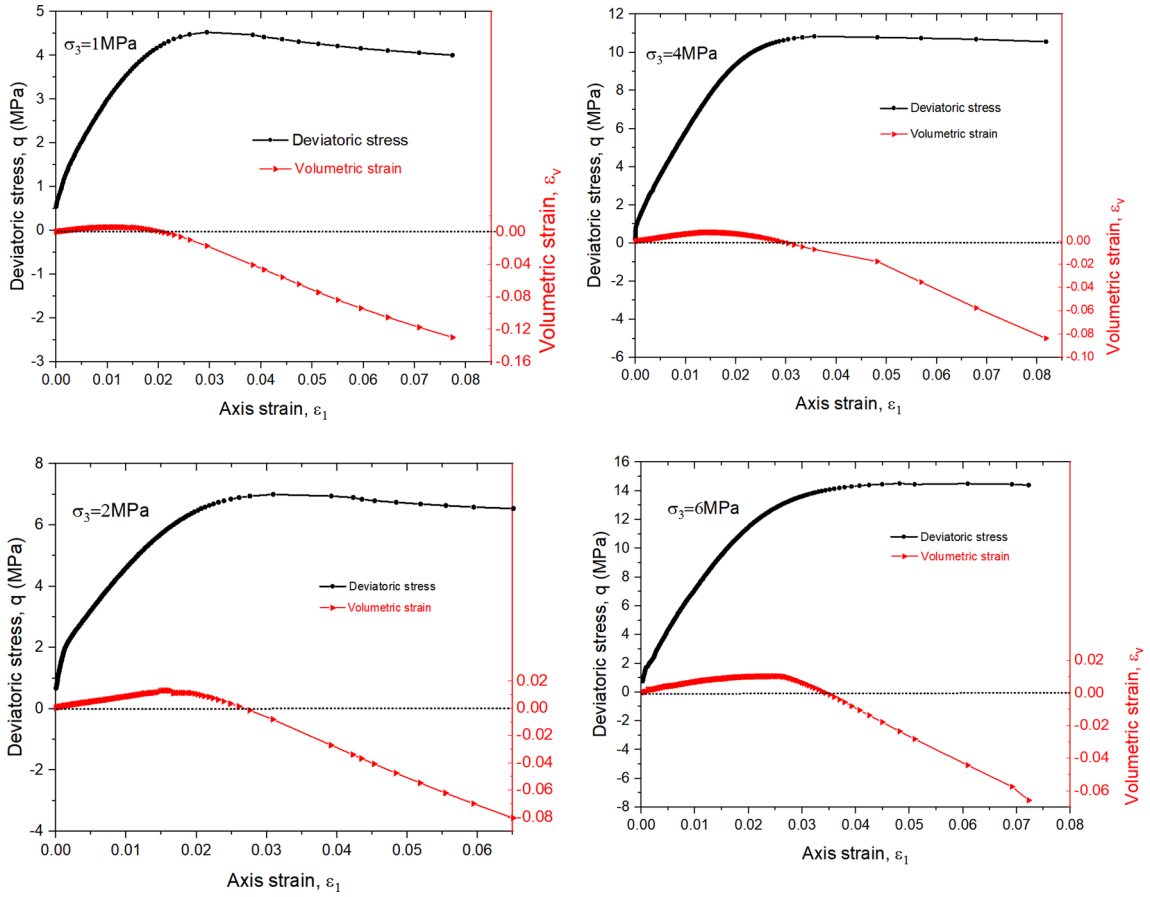

Fig. 4 Deviatoric stress and volumetric strain with respect to axial strain under different confining pressures for Group II

the deviatoric stress shows different trends for different tests. An obvious decrease trend is observed for the 2 MPa, 4 MPa confining tests in Group I and the 1 MPa, 2 MPa confining tests in Group II. For the 6 MPa confining test in Group I and the 4 MPa confining test in Group II, the deviatoric stress at the end of the test is smaller than the peak stress. The deviatoric stress shows a very gentle decrease trend. For the 8 MPa confining test in Group I and the 6 MPa confining test in Group II, the deviatoric stress does not drop at all and on the contrary an increase trend is observed.

In this study, the intermediate principal stress (σ_2) is equal to the minimum principal stress (σ_3) that is applied through the confining pressure. The volumetric strain is calculated as the sum of all the principal strains, $\varepsilon_v = \varepsilon_1 + 2\varepsilon_3$. The compaction of volume is noted as positive and the expansion of volume is noted as negative. For all of the tests, the volumetric strain shows positive first and then negative trends.

3.2 Relationship Between Axial Stress and Confining Stress

It is also noticed that the confining pressure has a positive impact to the maximum deviatoric stress (σ_p). The peak stress in each test is picked out and the relationship is plotted in Fig. 5. A good linear relationship between the confining stress and the maximum axial stress is observed. For rock or soil, it is widely accepted that the failure is introduced by the shear force. The Mohr–Coulomb criterion is used in this study to evaluate the strength of the specimens, which is expressed as:

$$\tau = c + \sigma \tan \varphi \tag{1}$$

where τ is the shear stress, σ is the normal stress, c is the cohesion of the specimen, φ is the internal friction angle.

Based on the Mohr–Coulomb criterion and the relationship between σ_1 and σ_3, the cohesion and internal friction angle can be written as:

$$\sigma_1 = M + N\sigma_3 \tag{2}$$

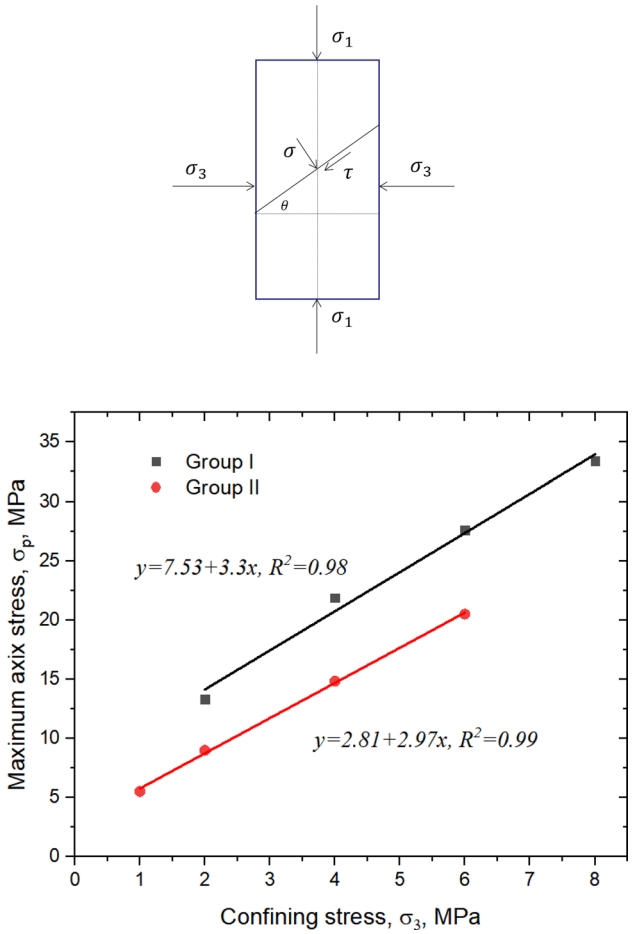

Fig. 5 Relationship between confining stress and maximum axial stress

Table 3 Young's modulus and Poisson's ratio

Confining pressure, MPa	Young's modulus, MPa	Poisson's ratio
Group I		
2	536	0.30
4	767	0.40
6	1141	0.32
8	1294	0.34
Group II		
1	301	0.45
2	485	0.27
4	613	0.38
6	745	0.38

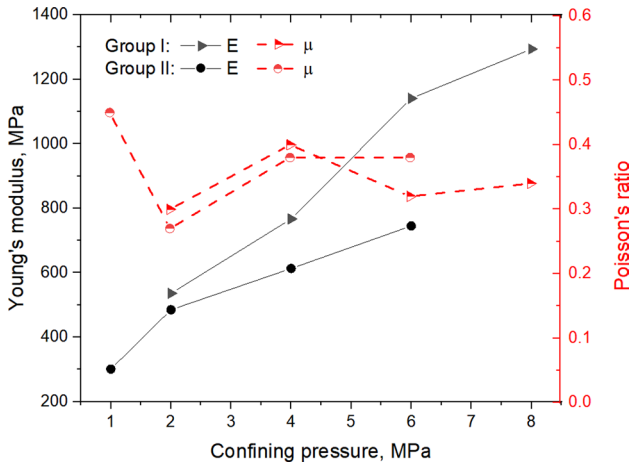

Fig. 6 Young's modulus and Poisson's ratio under different confining pressures

Table 2 Cohesion and internal friction angle for reconstituted coals

Sample	Cohesion, MPa	Internal friction angle, °
Group I	2.08	32.4
Group II	0.82	29.8

$$M = \frac{2c\cos\varphi}{1-\sin\varphi} \tag{3}$$

$$N = \tan^2\left(45° + \frac{\varphi}{2}\right) \tag{4}$$

The cohesion and internal friction angle of the samples are calculated and summarized in Table 2. It can be seen that the cohesions for the two groups are much different from each other, while the internal friction angles are very close (32.4° and 29.8°). The sample preparation process is of much importance for the mechanical properties. Young's modulus and Poisson's ratio are calculated based on the linear part of the stress–strain curve. For uniaxial compression test, Young's modulus is calculated as change in axial stress divided by change in axial strain and Poisson's ratio is calculated as negative change in radial strain divided by change in axial strain based on the linear part of the stress–strain curve. Under triaxial compression conditions, Young's modulus and Poisson's ratio can still be calculated through this method, but the axial strain is induced by three components: stress in x direction, stress in y direction and stress in z direction. So, the Generalized Hooke Law applies and Young's modulus and Poisson's ratio can be calculated as:

$$E = \frac{\sigma_1 - 2\mu\sigma_3}{\varepsilon_1} \tag{5}$$

$$\mu = \frac{B\sigma_1 - \sigma_3}{\sigma_3(2B-1) - \sigma_1} \tag{6}$$

where E and μ are Young's modulus and Poisson's ratio, respectively. $B = \varepsilon_3/\varepsilon_1$. Table 3 summarized Young's modulus and Poisson's ratio for specimens under different confining pressures. The variations are also plotted in Fig. 6. It can be seen that with the increase of the confining pressure, the Young's modulus shows an increase trend, while for the Poisson's ratio, there is no obvious trend. It should also be noted that under the same confining pressure conditions, the Young's modulus of Group I is higher than that of Group II. The external force also influences Young's modulus.

3.3 Stress–Dilatancy

At the end of each test, the coal sample was taken out of the triaxial cell and the failure profile of each sample was checked. The failure profile of the reconstituted coal is obviously different from that of the intact coal. Many researchers have reported that the shear failure is observed in reconstituted coal and the intact coal shows brittle character. Dilatancy of the sample is observed for the reconstituted coals. It is used to describe the volume increase during the shearing process. The dilatancy ratio, d, is defined as:

$$d = -\frac{d\varepsilon_v^p}{d\varepsilon_s^p} \tag{7}$$

$$d\varepsilon_s^p = \frac{2}{3}\left(d\varepsilon_1^p - d\varepsilon_3^p\right) \tag{8}$$

where $d\varepsilon_v^p$ and $d\varepsilon_s^p$ are the differential of plastic volumetric strain and plastic shear strain. $d\varepsilon_1^p$ and $d\varepsilon_3^p$ are the major and minor principal differential strain. As mentioned above, compression here is defined as positive, so when $d>0$, the specimen is in dilatant state, and when $d<0$, the specimen is in compression state. The dilatancy ratio with respect to the axial strain is shown in Fig. 7. It can be seen that for all test, the dilatancy ratio was negative in the early stage of the test. After that, the dilatancy ratio increases gradually and stables at a particular value, except for the 2 MPa confining test in Group I. The dilatancy ratio in this test drops to zero at the end of the test. The possible reason is that the specimen is completely destroyed by the external loading and it is in a granular material state. But from the deviatoric stress aspect, there is still existing residual stress. More explanations will be given in the discussion section.

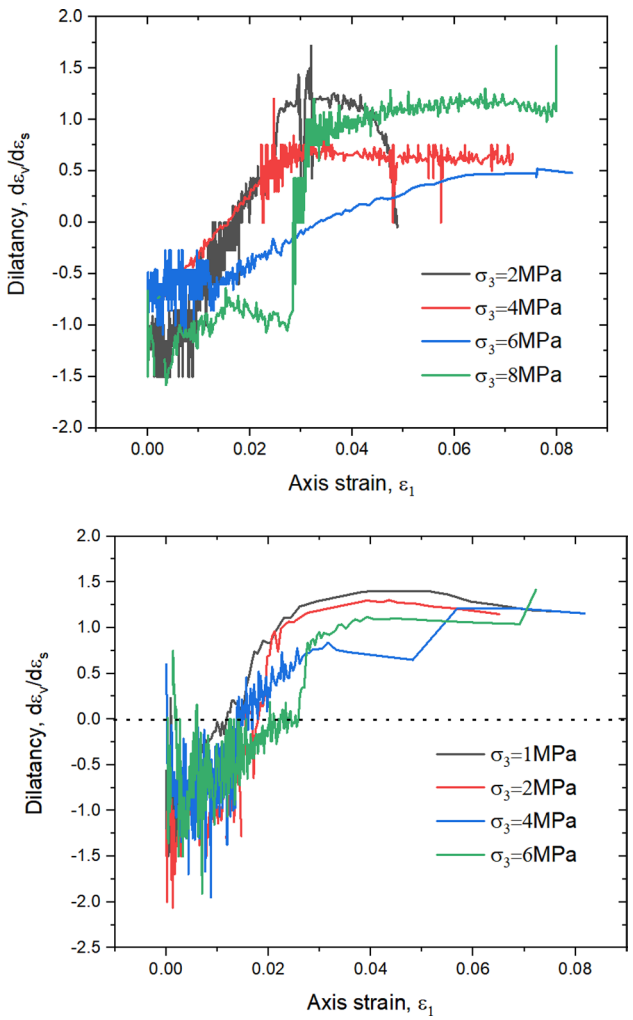

Fig. 7 Dilatancy ratio with respect to axial strain

4 Discussion

4.1 Consolidation and Over-consolidation

The term "consolidation" is used in soil mechanics. For soil grains, they are compacted by the in situ stress and the volume of the soil changes. For the reconstituted coal sample preparation process, it can also be defined as consolidation process of coal particles. The coal particles are loaded into the steel mold and being compacted by the upper loading force. From the testing results, it can be seen that the cohesion is much relevant to the external forces. The higher the external force, the higher is the cohesion.

From the deviatoric stress–axial strain curves, different trends are observed for different confining testing. With the increase of the confining pressure, when the peak stress is reached, the stress suddenly decrease effect becomes less significant. The normalized deviatoric stress, q/σ_3, with respect to the axial strain is shown in Fig. 8.

The normalized stress decrease percentage is calculated based on the stress state at the end of the test and the peak stress state, as written:

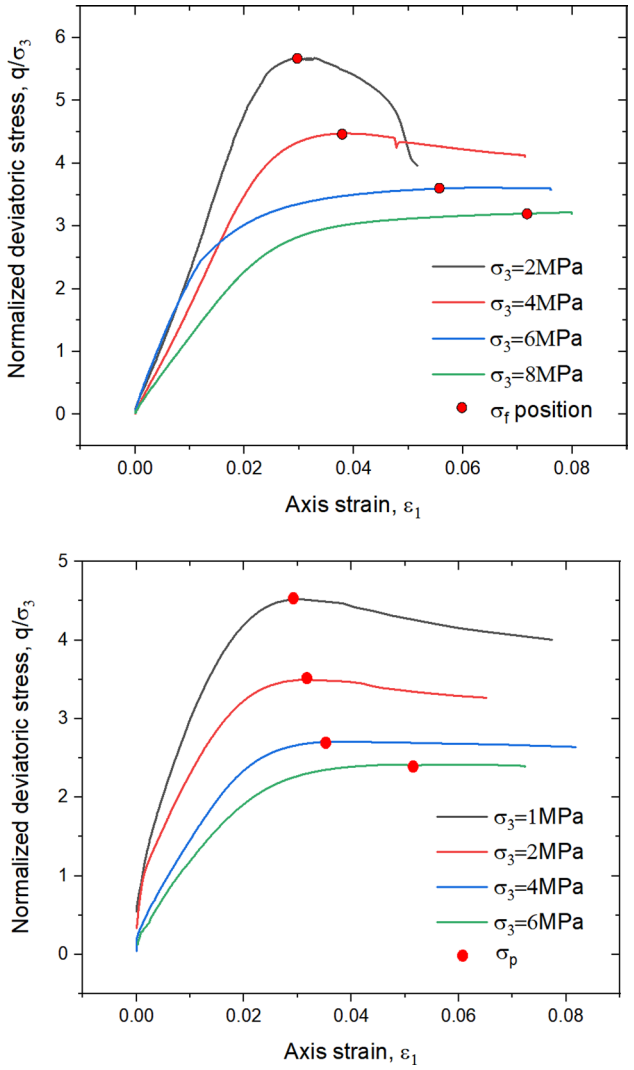

Fig. 8 Normalized deviatoric stress with respect to axial strain for different samples

$$\eta = \frac{N_p - N_r}{N_p} \times 100\% \tag{9}$$

where η is the normalized stress decrease percentage, N_p and N_r are the normalized stress at the peak state and at the end of the test, respectively. The normalized stress decrease percentage is shown in Fig. 9. It can be seen that with the increase of confining pressure, the deviatoric stress decreasing effect becomes less significant.

The mechanical properties of the clay are closely related to the stress history (Nygård et al. 2006). If the present stress is the maximum to which the clay has ever been experienced, the clay is defined as normal consolidation. If the stress magnitude of the consolidation process is greater than the current stress, it is experiencing over-consolidation. Figure 10 illustrates the mechanical features of normal

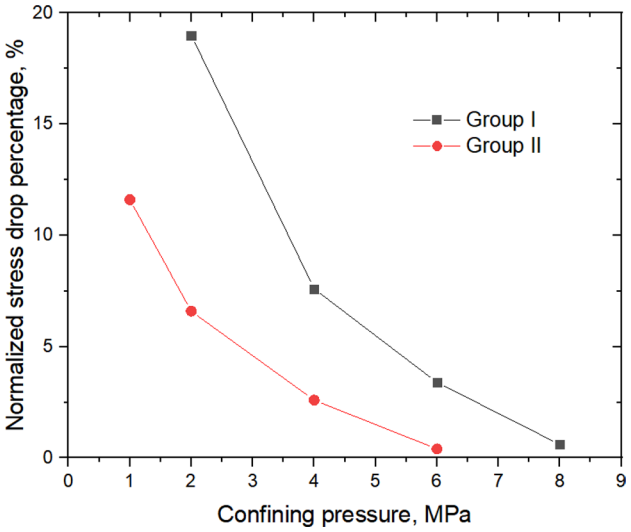

Fig. 9 Normalized stress decrease percentage with respect to confining pressure

consolidated soil and over-consolidated soil. For normal consolidated samples, the deviatoric stress increases gradually and an ultimate value is reached with the increasing of axial strain. No stress decreasing effect can be observed. For over-consolidated samples, the peak stress is obtained at relatively low strain and after that, stress decreasing effect is observed. The strain-softening effects are significant.

This is also suitable for the tests of reconstituted coal. In this study, the preparation of the reconstituted coals can be regarded as unsaturated-consolidated-drained process. Water is used as the additive (6 wt%) and is far from saturation. As illustrated in Fig. 9, with the increase of the confining pressure, the stress decreasing effects become weaker. In the 8 MPa confining test in Group I and 6 MPa confining test in Group II, the stress decrease ratios are − 0.04% and − 0.06%, respectively (the deviatoric stress increases rather than decreases). A conclusion can be easily drawn: the reconstituted coal samples are transforming from overconsolidation state to normal consolidation state. This feature of the reconstituted coal samples is closely related to the sample preparation process. Due to the limitation of sampling technique in the laboratory, the external forces are applied on the top end face of the specimen. The internal stress between the coal particles is largely reduced by the frictions between coal and mold. The actual molding force is significantly affected by the friction between the coal and the mold. It is shown that the consolidation force at the bottom of the cylinder is much reduced (Sun et al. 2020). Based on the testing results, it is inferred that the consolidation stresses for Group I and Group II are ranging between 6–8 MPa and 4–6 MPa, respectively. The over-consolidation ratio (OCR) is often used to quantify the stress state and it

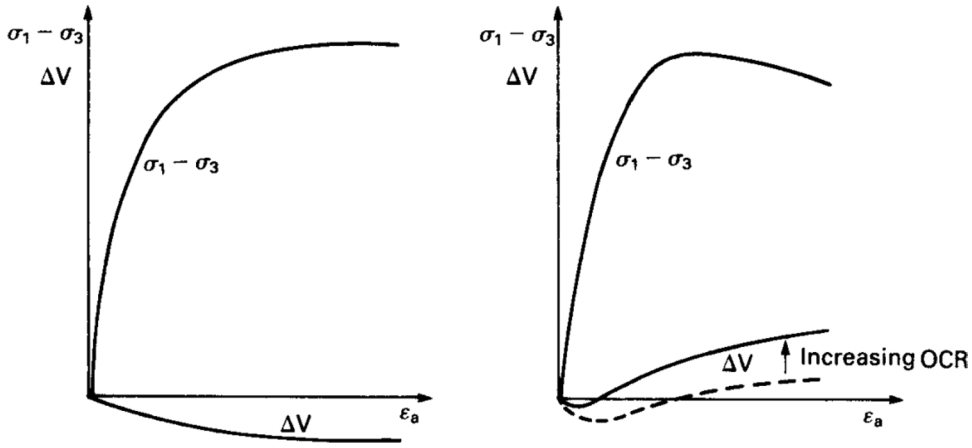

Fig. 10 Typical results from normal consolidated-drained and over-consolidated-drained tests (Craig 2004)

Table 4 Over-consolidation ratio for different confining pressure tests

Testing	OCR	Testing	OCR
2 MPa in Group I	3.5	1 MPa in Group II	5
4 MPa in Group I	1.75	2 MPa in Group II	2.5
6 MPa in Group I	1.17	4 MPa in Group II	1.25
8 MPa in Group I	0.875	6 MPa in Group II	0.83

is the ratio between the maximum stress (σ_M) in the past divided by the present stress (σ_{present}), $\text{OCR} = \frac{\sigma_M}{\sigma_{\text{present}}}$.

In this study, if the median of the range of the consolidation stress is taken as 7 MPa for Group I and 5 MPa for Group II, and the calculated OCR is summarized in Table 4.

Over-consolidation has impact on the shear and dilatancy behaviors of the samples, including soil and mudrocks (Nygård et al. 2006). From the testing results in this study, it can be regarded that the samples in Group I is consolidated in 7 MPa equivalent confining stress environment and the samples in Group II is consolidated in 5 MPa equivalent confining stress environment. This finding improves our understanding of reconstituted coals. Currently, the reconstituted coals are commonly used to represent the tectonic coals that exist in the geological zones. The reconstituted coals can only represent the coals that is in the same consolidation stress environment. The density, porosity and permeability are significantly influenced by the consolidation stress. So, in the future, appropriate preparation procedures of reconstituted coals are required.

4.2 Stress–Dilatancy Under Different Confining Stress

Dilatancy is used to describe the increase of volume during the failure process of dense sand or consolidated sample (Cuccovillo and Coop 1999). It is the same to the consolidated reconstituted coals. From the testing results, the cohesion is closely related to the applied external force. Bonds between coal particles are developed during the consolidation process. The coal grains are interlocked by the bond. This can be proven by the SEM images of the reconstituted coals. A bridge-like connection is developed between the coal particles and it is mainly contributing to the cohesion of the specimen. In the triaxial compression test, before the shear failure occurs, the interlocking or bonds need to be broken first and the interlocking effects are closely related to the OCR (Wang and Leung 2008). The breakage of the bonds between coal particles has two effects: the strength of the sample decreases; the volume of the sample, or dilatancy, increases. From the energy aspect, Cuccovillo and Coop (Cuccovillo and Coop 1999) found that the total work (ΔW) by the external force is converted into two components in the consolidated specimen: frictional loss (ΔW_f) and bond breakage (ΔW_b), as written:

$$\Delta W = \Delta W_f + \Delta W_b \tag{10}$$

For the triaxial compression testing, the work done by the external force mainly includes axial stress and the confining stress, so for a volume element, it is written as:

$$\Delta W = q \cdot d\varepsilon_s^p + p \cdot d\varepsilon_v^p \tag{11}$$

where q is the deviatoric stress, ε_s^p is the plastic shear strain, p is the mean stress, $p = (\sigma_1 + 2\sigma_3)/3$, ε_v^p is the plastic volume strain. The friction loss is proposed as:

$$\Delta W_f = Mp \cdot \mathrm{d}\varepsilon_s^p \tag{12}$$

where M is the critical state stress ratio (friction at the critical state, it is referred to the final stress state or residual stress state). If the bonds between coal particles are completely destroyed, the stress ratio at the residual stress state, M is only controlled by the coal particle surface properties (the shape profile, surface roughness, etc.). The Eq. (10) can be written as:

$$q \cdot d\varepsilon_s^p + p \cdot d\varepsilon_v^p = Mp \cdot d\varepsilon_s^p + \cdot W_b \tag{13}$$

$$\frac{q}{p} = M - \frac{d\varepsilon_v^p}{d\varepsilon_s^p} + \frac{\Delta W_b}{p d\varepsilon_s^p} \tag{14}$$

It can be seen that the stress ratio is determined by three components: the critical stress ratio, dilatancy and the bond breakage. The dilatancy and bond breakage are correlated with each other.

From Fig. 7, it can be seen that the dilatancy of each test becomes stable except for the test of 2 MPa confining stress in Group I. The final dilatancy ratio for Group I is ranging between 0.5 and 1.25. The final dilatancy ratio for Group II is ranging between 1 and 1.5. The dilatancy effect is positively related to the bond breakage. Based on the Eqs. (10–14), the dilatancy ratio value indicates the bond breakage. It can be concluded that bond breakage continuously occurs at the end of the test. The coal specimens are experiencing stable dilatancy failure process (otherwise the dilatancy ratio decreases to zero). It is also observed that the cohesion hinders dilatancy. The Group I is of higher cohesion than the Group II. The average dilatancy ratio of the Group I is lower than that of the Group II.

4.3 Failure Mechanisms of Reconstituted Coals

The failure process of intact coals is extensively investigated under uniaxial/triaxial confining stress conditions (Mishra and Nie 2013). It is commonly regarded that the failure process of intact coal is very similar to that of rock (Du and Wang 2019; Meng et al. 2020; Zhao et al. 2021a). Figure 11 shows the deviatoric stress with respect to axial strain of the intact coal which was tested by the same triaxial testing rig. Obvious shear failure occurred when the failed sample was investigated after the test. Even though the strength of coal is much lower than rock strength, the coal is still regarded as brittle material under the testing confining pressures. That means the intact coal is still very stiff and the failure mechanism of rock can still be used to describe the intact coal (not tectonic coal) failure process.

For the brittle failure of rock/intact coal, there are mainly four stages during the course of failure (Li et al. 2017). (1) Crack closure stage. The original cracks exist in the specimen and are compacted by the external forces. (2) Stress linear increase stage. The initial existing crack closure stage is followed by a stress linear increase stage which includes the elastic deformation and crack steady increase. (3) Crack propagation stage. When the axial stress reaches the crack initiation stress σ_{ci}, the stable crack propagation is developed. When the axial stress reaches σ_{cd}, unstable crack growth and irrecoverable deformations begin to develop until the peak stress σ_p is reached. (4) Post-failure stage. After the stress peak, it comes into the post-failure stage, with the axial stress decrease and residual stress obtained.

Confining pressure impacts the properties of rock. It not only influences the strength (maximum axial stress) of the rock, but also affects the brittle–ductile characteristics. It is regarded that the rock transforms from brittle material to ductile material with increasing of confining pressure. Due to the lower strength of coal than rock, the transforming stress for intact coal would be lower. In this study, the

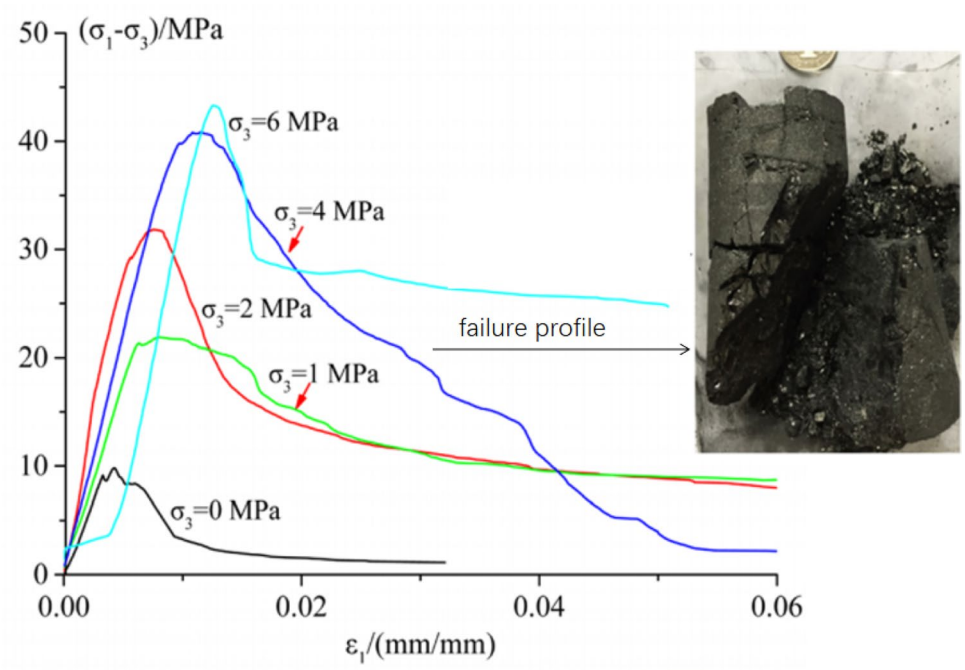

Fig. 11 Deviatoric stress with respect to axial strain under different confining stress for intact coal (Tu et al. 2019)

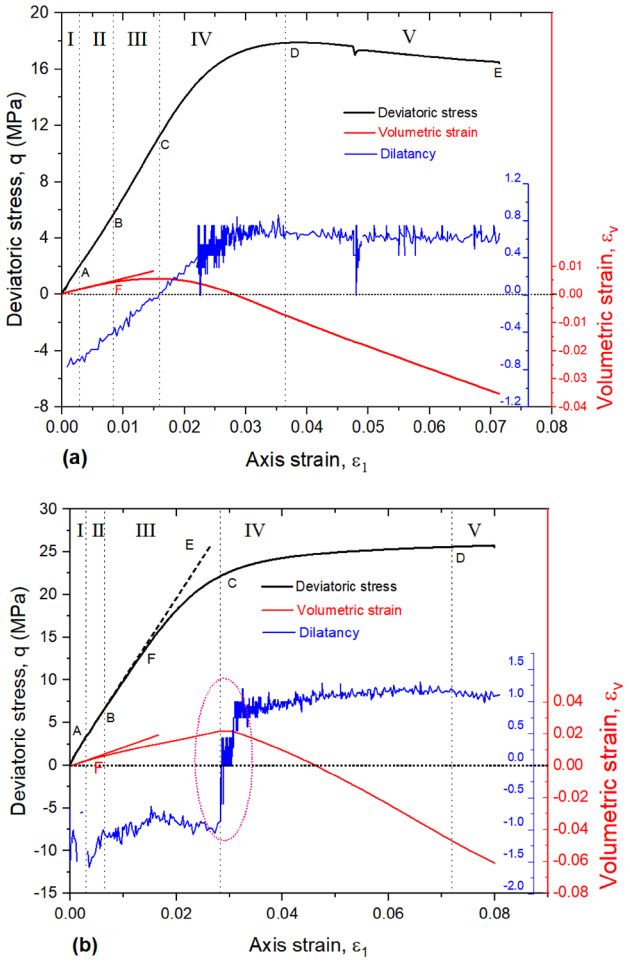

Fig. 12 Failure process of reconstituted coals under different confining pressures **a** 4 MPa confining pressure in Group I **b** 8 MPa confining pressure in Group I

reconstituted coal shows brittle–ductile transient state in low confining tests (2 MPa, 4 MPa confining in Group I and 1 MPa, 2 MPa confining in Group II). It becomes ductile when relative high confining pressures are applied (6 MPa, 8 MPa confining in Group I and 4 MPa, 6 MPa confining in Group II).

The failure behaviors are different for the reconstituted coals under different confining pressures (Chen et al. 2014; Song et al. 2021). Based on the stress curve, volumetric curve (Figs. 3 and 4) and the dilatancy curve (Fig. 7), the failure process of reconstituted coal is divided into five stages. But for the over-consolidation scenario and normal consolidation scenario, the failure processes are different. The reconstituted coal failures of 4 MPa confining in Group I and 8 MPa confining in Group I are taken as an example for illustration.

In 4 MPa confining of Group I test, the reconstituted coal is regarded under over-consolidation stress state, as shown in Fig. 12a. It is similar to the intact coal failure process. In *0A* stage, the original facture or macropores are closed. In *AB* stage, the specimen is experiencing the elastic deformation process. For the volumetric strain curve, it is a linear line until it deviates from linearity at point *F*. In *BC* stage, stable fractures are developing. The volumetric strain is the combination of the compaction and the volume dilatancy, and the specimen is still compaction dominate ($\varepsilon_{\text{compaction}} > \varepsilon_{\text{dilatancy}}$). At point *C*, the maximum volumetric strain is obtained and after that, it goes into *CD* stage whereby unstable fractures develop and irrecoverable deformation occurs. The dilatancy effect is stronger than the compaction effect and the specimen shows a tendency of expansion. At point *D*, the maximum stress is reached. In *DE* stage, the strain-softening effect appears and there is a stress decreasing trend.

It can be seen that the failure behavior of over-consolidated reconstituted coal is similar to that of rock/intact coal. It should be noted the precondition is that the bond breakage stress is larger than the internal friction force. Specifically, the threshold limit stress for bond breakage (σ_{bb}) is larger than the maximum friction stress (σ_{mf}). As mentioned above in Eq. (10), during the failure process, it is required to overcome the bond resistance and internal friction resistance. The maximum friction stress is affected by the confining pressure. Under a certain confining pressure (σ_3), the maximum friction stress (σ_{mf}) is a specific fixed value. With the increase of the axial stress (σ_1), the internal friction force (f) is:

$$f = \begin{cases} 0 < k\sigma_n < \sigma_{mf}, \text{static friction force} \\ \sigma_{mf}, \text{kinetic friction force} \end{cases} \tag{15}$$

where k is the internal friction force coefficient that is related to the material properties, σ_n is the normal stress applied on the internal plane and it is calculated from the confining pressure and the axial stress. The kinetic friction force is the internal friction force when new fractures are formed and two fracture surfaces are moving with respect to one another.

The bonds between coal particles are stronger for higher external-force applied reconstituted coals. The bond strength is higher for the stronger bonds coal (Wang and Leung 2008). Usually, it is regarded that the bond strength of rock is much higher than the internal friction force under low confining pressure. For a reconstituted coal specimen, the strength of the bond as well as the internal friction force correspond to the confining pressure are also dependent on the external applied force during specimen preparation. If the current confining pressure is lower than the specimen consolidation pressure (over-consolidation scenario), the strength of bond is higher than the internal friction force. For normal consolidation scenario with the current confining pressure higher than the specimen consolidation pressure, the bond strength is weaker than the maximum internal friction force. Therefore, the failure

behaviors of normal consolidated coal are different from that of over-consolidated coal.

As shown in Fig. 12b, the *0A* stage and the *AB* stage are the same to that of over-consolidated coal. The specimen is compacted by the external loadings and then followed by an elastic deformation. In stage *BC*, new fractures are developed as the linear line deviates from linearity in the volumetric strain curve at point *F*. In this stage, the volumetric strain still increases, which means that the compaction effect is stronger than the new fracture induced expansion effect. But from the stress–strain curve, it is not increasing linearly and the stress–strain curve is under the tangent line *BE*. That means, even though the specimen is in compaction state, the internal factures weaken the strength of the specimen. Substantial bond breakage is the main reason for this. At point *C*, the maximum volumetric strain is reached and the dilatancy ratio changes from negative to positive. In stage *CD*, dilatancy effect appears, which means the specimen expansion effect is stronger than the compaction effect. It should also be noted that the dilatancy ratio increases sharply from 0 to 1.0 when the axial strain is between 0.28 and 0.32. It can be concluded that the specimen expands extensively. This is also a reflection of substantial bond breakage in *FC* period. The coal particles are detached from each other but they are still compacted by the confining pressure. At this moment, many parts of the specimen can be regarded as granular materials due to the bond-breakage effect. In stage *CD*, the bonds are continuously being damaged and the dilatancy ratio is stable between 0.9 and 1.1. Under the current testing conditions, the specimen would not be completely failed (all bonds are broken). So the strain-softening effect is difficult to be observed, which is also observed in clay failure process.

From the energy aspect, the deviatoric stress is contributing to two effects: bond breakage and internal friction resistance which are represented in Eq. (10). As shown in Fig. 13, for normal consolidated coal, the stress magnitude order is: $\sigma_{bb} < \sigma_{mf}$. With the increase of the deviatoric stress, the shear stress applied on the coal particle exceeds the bond strength σ_{bb}, so the specimen is experiencing bond breakage without any slippage on the internal weak plane, as shown the stage *FC* in Fig. 12b. The stress state in this stage is: $\sigma_{bb} < \tau < \sigma_{mf}$. When the deviatoric stress is continuously increasing, the shear stress on the internal plane overcomes the maximum friction force, $\sigma_{bb} < \sigma_{mf} < \tau$. The specimen shows expansion and slippage occurred inside of the specimen. It comes into the stage *CD* in Fig. 12b. Both bond breakage and internal slippage are happening in this period.

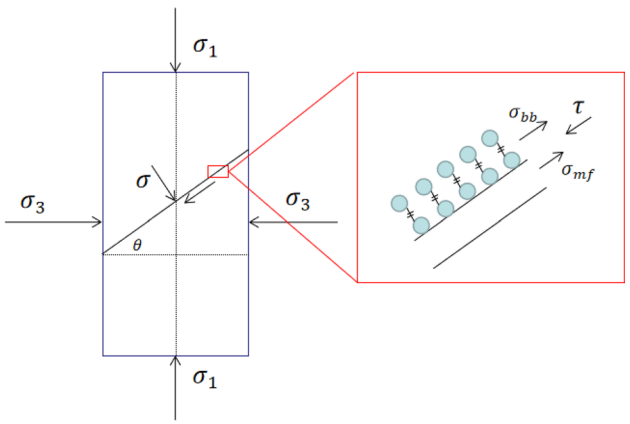

Fig. 13 Schematic diagram of the failure of bond and internal friction

4.4 Effects on Coal and Gas Outburst

The three key elements of coal and gas outburst are high gas content, high stress and geological structure (Beamish and Crosdale 1998; Doyle 2002; Gray 2006; Kissell and Iannacchione 2014). The integration of these three effects can lead to the occurrence of an outburst. From this study, the roles of these three factors are clear. The bonds in structure coals or tectonic coals are much weaker than the bonds in intact coals. The required energy for bond breakage is much lower for tectonic coals. That means, under current mining conditions, the in situ stress environment can meet this requirement for tectonic coal breakage. In situ stress mainly contributes to the deformation of coal. It not only shears the coal and causes slippage, but also breaks the bonds between coal grains. Coal and rock would transform from brittle materials to ductile materials in high in situ stress environment (Kim et al. 2020; Nygård et al. 2006). Due to the low strength of coal, the transformation is possible in current mining depth. During the excavation of roadways, the coal seam is in yielded state near the heading face. Especially for the tectonic coals, the bonds between coal particles are broken. The yielded coals are compacted by the surrounding stress. If the adjacent coal is disturbed or mined out, the yielded coals will fail or collapse. In this scenario, if gas exists in the yielded coal, the expansion energy of gas would be released and hence, an outburst event happens. In this process, gas mainly plays the role of coal particle transportation. It should be noted that only free gas has the potential to transport coal particles. The high in situ stress breaks the coal into small particles. If the coal originally contains adsorbed gas, the sudden breakage of coal would result in gas desorption from this small coal particles. Many researchers have pointed out that this small coal particles contain micropores that are the main sites for gas adsorption. New volumes are generated during the failure process and adsorbed gas tend to desorb from the internal surface of pores. With decrease of the coal size, the gas diffusion rate would sharply increase and large volume of free-state gas accumulates in the void space.

5 Conclusion

Two groups of reconstituted coals were prepared in the laboratory under different external forces. Triaxial texts were conducted under different confining pressures. The deviatoric stress, volumetric strain, axial strain and dilatancy ratio were analyzed. The failure behaviors of the reconstituted coals are compared with the intact coals. New insights into the failure mechanisms are obtained based on the testing results. The new findings in this study significantly improve our understanding of the interactions between coal particles and in situ stress. It can also provide guidance for laboratory studies of tectonic coals. The main conclusions are summarized as follows:

(1) The mechanical properties of reconstituted coal are highly related to the specimen preparation process. The cohesion has positive relationship with the external molding force while the internal friction angle is much less affected by this force. The cohesion of the 200 KN external force generated specimen is 2.08 MPa. When the external force is reduced to 100 KN, the cohesion is 0.82 MPa. The internal friction angles for 200 KN and 100 KN external forces are 32.4° and 29.8°, respectively. The friction angle is only affected by the coal particle surface properties.

(2) The reconstituted coal shows brittle–ductile transient characteristic in relative low confining pressure test. As stated in Sect. 4.3, the failure process of tectonic coal mainly includes two parts: bond breakage and internal surface movement with respect to one another. For one tectonic coal specimen in the laboratory testing, the strength of the bond is fixed and is only affected by the sample preparation parameters. But for the internal surface movement, it is controlled by the confining pressure. With the increase of confining pressure, it transforms to ductile material. The stress decreasing effect becomes weaker when the confining pressure exceeds a certain value. For high confining pressure test (the strength of bond is lower than the internal surface movement force), in the loading process, the bond breakage happens before the internal surface movement. With the bond breakage, many new internal surfaces are formed. The specimen shows dilatancy effect. There is no stress decreasing effect and no strain-softening effect observed.

(3) The over-consolidation ratio (OCR) can be used as an index to evaluate the specimen behavior. At present, the reconstituted coal is often used to study the failure behavior of tectonic coal. Based on the OCR index, the relationship between reconstituted coal and in situ coal seam is established. The reconstituted coal can be used to represent the specific in situ tectonic coal more accurately.

(4) The dilatancy ratio is stable when the maximum deviatoric stress is reached. The specimen is expanding steadily due to the coal particles bond breakage. The cohesion hinders the dilatancy effects. The maximum deviatoric stress mainly contributes to the three factors: friction effects, dilatancy and bond breakage.

(5) The failure behaviors of normal consolidated coal and over-consolidated coal are different. The failure process of the over-consolidated reconstituted coal is similar to the intact coals. Before the yielded of the specimen, it behaves like intact coal. Bond breakage is not obvious. After the yielding, bond breakage gradually increases. When the deviatoric stress reaches the peak value, the maximum dilatancy ratio is obtained and bond breakage effect also reaches the peak. After that, bond breakage occurs continuously with the strain-softening effect. For normal consolidated coal, the bond breakage stress is lower than the maximum internal friction force, $\sigma_{bb} < \sigma_{mf}$. The bond breakage happens earlier than the internal slippage $\sigma_{bb} < \tau < \sigma_{mf}$. Before the volumetric strain reaches the maximum value (maximum compaction state), the internal bond breakage weakens the specimen strength. When the shear stress exceeds the maximum internal friction force, $\sigma_{bb} < \sigma_{mf} < \tau$, the internal slippage happens and the specimen expands sharply with extensive dilatancy occurring. No strain-softening effect is observed.

Acknowledgements Financial supports from the National Natural Science Foundation of China (No. 51874294, No. 52004277) are acknowledged.

Author contributions JL: conceptualization, methodology, investigation, writing—original draft, funding acquisition. YC: supervision, funding acquisition, resources, methodology. QL: validation, investigation, data curation. QT: data curation. TR: supervision, writing—review and editing.

Declarations

Conflict of interest The authors report no declarations of interest.

References

Anyim K, Gan Q (2020) Fault zone exploitation in geothermal reservoirs: production optimization, permeability evolution and induced seismicity. Adv Geo-Energy Res 4:1–12

Beamish BB, Crosdale PJ (1998) Instantaneous outbursts in underground coal mines: an overview and association with coal type. Int J Coal Geol 35:27–55

Chen H-D, Yuan-Ping C, Zhou H-X, Li W (2013) Damage and permeability development in coal during unloading. Rock Mech Rock Eng 46:1377–1390
Chen H, Cheng Y, Ren T, Zhou H, Liu Q (2014) Permeability distribution characteristics of protected coal seams during unloading of the coal body. Int J Rock Mech Min Sci 71:105–116
Chen M-Y, Cheng Y-P, Zhou H-X, Wang L, Tian F-C, Jin K (2017) Effects of igneous intrusions on coal pore structure, methane desorption and diffusion within coal, and gas occurrence. Environ Eng Geosci 23:191–207
Cheng Y, Pan Z (2020) Reservoir properties of Chinese tectonic coal: a review. Fuel 260:116350
Craig RF (2004) Craig's soil mechanics. CRC Press
Cuccovillo T, Coop MR (1999) On the mechanics of structured sands. Géotechnique 49:741–760
Dong J, Cheng Y, Hu B, Hao C, Tu Q, Liu Z (2018) Experimental study of the mechanical properties of intact and tectonic coal via compression of a single particle. Powder Technol 325:412–419
Doyle R (2002) Geological Structures in Relation to Outburst Events
Du F, Wang K (2019) Unstable failure of gas-bearing coal-rock combination bodies: Insights from physical experiments and numerical simulations. Process Saf Environ Prot 129:264–279
Fan C, Li S, Elsworth D, Han J, Yang Z (2020) Experimental investigation on dynamic strength and energy dissipation characteristics of gas outburst-prone coal. Energy Sci Eng 8:1015–1028
Frodsham K, Gayer RA (1999) The impact of tectonic deformation upon coal seams in the South Wales coalfield, UK. Int J Coal Geol 38:297–332
Gray I (2006) Coal mine outburst mechanism, thresholds and prediction techniques. ACARP Report C 14032
Harvey C, Singh R (1998) A review of fatal outburst incidents in the Bulli seam
Jia D, Qiu Y, Li C, Cai Y (2019) Propagation of pressure drop in coalbed methane reservoir during drainage stage. Adv Geo-Energy Res 3:387–395
Jin K, Cheng Y, Liu Q, Zhao W, Wang L, Wang F, Wu D (2016) Experimental investigation of pore structure damage in pulverized coal: implications for methane adsorption and diffusion characteristics. Energy Fuels 30:10383–10395
Karacan CÖ, Ruiz FA, Cotè M, Phipps S (2011) Coal mine methane: a review of capture and utilization practices with benefits to mining safety and to greenhouse gas reduction. Int J Coal Geol 86:121–156
Kim B-H, Walton G, Larson MK, Berry S (2020) Investigation of the anisotropic confinement-dependent brittleness of a Utah coal. Int J Coal Sci Technol 8:274–290
Kissell FN, Iannacchione AT (2014) Gas outbursts in coal seams. Coal bed methane: from prospect to pipeline, p 177
Lama RD, Bodziony J (1998) Management of outburst in underground coal mines. Int J Coal Geol 35:83–115
Li D, Sun Z, Xie T, Li X, Ranjith PG (2017) Energy evolution characteristics of hard rock during triaxial failure with different loading and unloading paths. Eng Geol 228:270–281
Liu Q, Cheng Y, Jin K, Tu Q, Zhao W, Zhang R (2017) Effect of confining pressure unloading on strength reduction of soft coal in borehole stability analysis. Environ Earth Sci 76:173. https://doi.org/10.1007/s12665-017-6509-9
Liu Q, Zhang K, Zhou H, Cheng Y, Zhang H, Wang L (2018) Experimental investigation into the damage-induced permeability and deformation relationship of tectonically deformed coal from Huainan coalfield, China. J Nat Gas Sci Eng 60:202–213
Meng Q-B, Liu J-F, Ren L, Pu H, Chen Y-L (2020) Experimental study on rock strength and deformation characteristics under triaxial cyclic loading and unloading conditions. Rock Mech Rock Eng 54:777–797
Mishra B, Nie D (2013) Experimental investigation of the effect of change in control modes on the post-failure behavior of coal and coal measures rock. Int J Rock Mech Min Sci 60:363–369
Nygård R, Gutierrez M, Bratli RK, Høeg KJM, Geology P (2006) Brittle–ductile transition, shear failure and leakage in shales and mudrocks. Marine Petrol Geol 23:201–212
Qu Z, Wang GGX, Jiang B, Rudolph V, Dou X, Li M (2010) Experimental study on the porous structure and compressibility of tectonized coals. Energy Fuels 24:2964–2973
Ranjith PG, Shao SS, Viete DR, Jaysinge D (2012) Carbon dioxide storage in coal: reconstituted coal as a structurally homogeneous substitute for coal. Int J Coal Prep Util 32:265–275
Skoczylas N, Dutka B, Sobczyk J (2014) Mechanical and gaseous properties of coal briquettes in terms of outburst risk. Fuel 134:45–52
Song H, Zuo J, Liu H, Zuo S (2021) The strength characteristics and progressive failure mechanism of soft rock-coal combination samples with consideration given to interface effects. Int J Rock Mech Min Sci 138:104593
Sun Y, Li G, Zhang J, Xu J (2020) Failure mechanisms of rheological coal roadway. Sustainability 12:2885
Tu Q, Cheng Y, Ren T, Wang Z, Lin J, Lei Y (2019) Role of tectonic coal in coal and gas outburst behavior during coal mining. Rock Mech Rock Eng 52:4619–4635
Wang YH, Leung SC (2008) Characterization of cemented sand by experimental and numerical investigations. J Geotech Geoenviron Eng 134:992–1004
Wold MB, Connell LD, Choi SK (2008) The role of spatial variability in coal seam parameters on gas outburst behaviour during coal mining. Int J Coal Geol 75:1–14
Wu S, Li B, Chu J (2021) Stress-dilatancy behavior of MICP-treated sand. Int J Geomech 21:04020264
Yu S, Bo J, Ming L, Chenliang H, Shaochun X (2020) A review on pore-fractures in tectonically deformed coals. Fuel 278:118248
Zhao H, Liu C, Huang G (2021a) Dilatancy behaviour and permeability evolution of sandstone subjected to initial confining pressures and unloading rates. R Soc Open Sci 8:201792
Zhao P, Zhuo R, Li S, Shu C-M, Jia Y, Lin H, Chang Z, Ho C-H, Laiwang B, Xiao P (2021b) Fractal characteristics of methane migration channels in inclined coal seams. Energy 225:120127